ELSEVIER

Biochimica et Biophysica Acta 1506 (2001) 89–102

BIOCHIMICA ET BIOPHYSICA ACTA
BBA

www.bba-direct.com

Analysis of suppressor mutation reveals long distance interactions in the bc_1 complex of *Saccharomyces cerevisiae*

Gaël Brasseur [a,*], Jean-Paul Di Rago [b], Piotr P. Slonimski [c], Danielle Lemesle-Meunier [a]

[a] *Laboratoire de Bioénergétique et Ingénierie des Protéines, CNRS, 31 ch. J. Aiguier, 13402 Marseilles Cedex 20, France*
[b] *Institut de Biochimie et Génétique Cellulaires, CNRS, 1 rue Camille Saint-Saëns, 33077 Bordeaux Cedex, France*
[c] *Centre de Génétique Moléculaire, CNRS, 91198 Gif-sur-Yvette cedex, France*

Received 27 February 2001; received in revised form 27 April 2001; accepted 2 May 2001

Abstract

Four totally conserved glycines are involved in the packing of the two cytochrome *b* hemes, b_L and b_H, of the bc_1 complex. The conserved glycine 131 is involved in the packing of heme b_L and is separated by only 3 Å from this heme in the bc_1 complex structure. The cytochrome *b* respiratory deficient mutant G131S is affected in the assembly of the bc_1 complex. An intragenic suppressor mutation was obtained at position 260, in the ef loop, where a glycine was replaced by an alanine. This respiratory competent revertant exhibited a low bc_1 complex activity and was affected in the electron transfer at the Q_P site. The k_{min} for the substrate DBH_2 was diminished by an order of magnitude and EPR spectra showed a partially empty Q_P site. However, the binding of the Q_P site inhibitors stigmatellin and myxothiazol remained unchanged in the suppressor strain. Optical spectroscopy revealed that heme b_L is red shifted by 0.8 nm and that the E_m of heme b_L was slightly increased (+20 mV) in the revertant strain as compared to wild type strain values. Addition of a methyl group at position 260 is thus sufficient to allow the assembly of the bc_1 complex and the insertion of heme b_L despite the presence of the serine at position 131. Surprisingly, reversion at position 260 was located 13 Å away from the original mutation and revealed a long distance interaction in the yeast bc_1 complex.

Keywords: bc_1 complex; Revertant; Long distance interaction; Heme b_L; Quinol binding; *Saccharomyces cerevisiae*

1. Introduction

The cytochrome bc_1 complex (known as the b_6f complex in chloroplasts and cyanobacteria) is a key component of the respiratory and photosynthetic electron transfer chains (see [1–3] for reviews). It is present in the cytoplasmic membrane of bacteria and in the inner mitochondrial membrane of eukaryotes and catalyzes the oxidation of hydroquinone linked to the reduction of cytochrome (cyt) *c*. This electron transfer is coupled to a vectorial translocation of protons across the membrane and is best described

Abbreviations: cyt, cytochrome; b_L, low potential cyt *b* heme; b_H, high potential cyt *b* heme; DB, 2,3-dimethoxy-5-methyl-6-decyl-1,4-benzoquinone; DBH_2, reduced form of DB; Q_P, ubiquinol oxidation site on the positive side of the inner mitochondrial membrane; Q_N, ubiquinone reduction site on the negative side; EPR, electron paramagnetic resonance; E_h, ambient redox potential; E_m, equilibrium redox midpoint potential; WT, parental strain

* Corresponding author. Fax: +33-4-91-16-45-63.
E-mail address: brasseur@ibsm.cnrs-mrs.fr (G. Brasseur).

0005-2728/01/$ – see front matter
PII: S0005-2728(01)00186-4

by the Q cycle mechanism [4–6]. All bc_1 complexes, from bacteria to higher eukaryotes, contain three subunits carrying four prosthetic groups: a monohemic cyt c_1, a FeS Rieske protein with a [2Fe–2S] cluster, a dihemic cyt b with a low potential b_L heme ($E_{m,7} = -50$ mV) located on the positive side of the membrane and a high potential b_H heme ($E_{m,7} = +90$ mV) located on the negative side of the membrane. In eukaryotic cells, in addition to these three totally conserved subunits, as many as eight additional subunits are found whose functions are poorly understood [7].

Several three-dimensional structures of eukaryotic bc_1 complexes have been obtained in the past few years in the presence or absence of different inhibitors [8–11]; this allows combined functional and structural analyses of mutants and revertants in the bc_1 complex subunits. Analyses of the different structures suggest that the extrinsic domain of the FeS Rieske protein carrying the [2Fe–2S] cluster may undergo a rotation between a position close to cytochrome b (proximal conformation or b state) and a position close to cytochrome c_1 (distal conformation or c_1 state), thus providing a rational explanation for the incompatibility of the distances and the rate of electron transfer between the redox centers [8–11]. Results obtained from mutagenesis experiments have confirmed this hypothesis [12–15]. Very recently, Hunte et al. solved the bc_1 complex structure of the yeast *Saccharomyces cerevisiae* at 2.3 Å, including water molecules [16]. Cytochrome b is an integral membrane protein with eight transmembrane helices and is a central component for quinol oxidation and inhibitor binding. According to the modified Q cycle [4–6,17], electrons are delivered into two bifurcated pathways at the Q_P site (on the positive side of the membrane): the first electron from quinol is transferred to the FeS Rieske protein (in the so-called high potential electron transfer pathway to cyt c_1 and the soluble cyt c) resulting in the formation of an unstable semiquinone which then transfers the second electron to hemes b_L and b_H (in the so-called low potential pathway) across the membrane. At the Q_N site, on the negative side of the membrane, quinone is reduced to semiquinone. Two molecules of ubiquinol at the Q_P site are thus required to reduce a quinone to quinol at the Q_N site. Several mechanistic models have been proposed on the basis of the Q cycle to account for the bifurcated electron transfer at the Q_P site [18–23].

Four totally conserved histidines are axial ligands for hemes b_L and b_H, and are located in the transmembrane helices B and D. Additionally, Tron et al. [24] proposed that four totally conserved glycines, present in the transmembrane helices A (glycines 33 and 47) and C (glycines 117 and 131) and separated by 13 amino acids in each helix (such as is the case of the four histidine ligands), may be important in the packing of hemes b_L and b_H. This proposal has been confirmed by analysis of the mitochondrial bc_1 complexes structures [8–10], in which the four glycines are symmetrically positioned close to either b_L or b_H hemes. Mutants of two of these glycines have been obtained at position G33 (yeast numbering) in both *S. cerevisiae* [25,26] and *Rhodobacter sphaeroides* [27], as well as at position G131 in *S. cerevisiae* [28] and *Rhodobacter capsulatus* [29]. Rather small amino acids, such as glycine or alanine, are required at these positions to allow correct assembly and function of the complex. Thus, glycines have been shown to be crucial in the packing of hemes b_L and b_H. The conserved glycine 131 is separated by only 3 Å from heme b_L in the bovine bc_1 complex structure.

In the present study, we investigated the possibility of obtaining second site suppressor mutations from the G131S mutant and undertook the biochemical and biophysical characterization of such a revertant. From the respiratory deficient mutant G131S, which has a bc_1 complex with an assembly defect, only one intragenic suppressor mutation distinct from the wild type glycine was found at position 260, in the ef loop, where a glycine was replaced by an alanine. This revertant restored the assembly of the bc_1 complex but exhibited a low bc_1 complex activity. It was shown to be affected mainly at the Q_P site, with a modified interaction with the substrate quinol. Surprisingly, reversion in position 260 occurred 13 Å away from the original mutation in position 131. This study reveals, for the first time, that a mutation at one of the totally conserved glycines at the end of the transmembrane helix C can be compensated by a long distance suppressor mutation in the non-transmembrane ef loop of cyt b. These results will be

presented with respect to the bc_1 complex structure and a possible explanation for this long distance interaction will be discussed.

2. Materials and methods

2.1. Strains

The original *rho*$^+$ *mit*$^-$ cytochrome *b* deficient mutant 777-3A/W7 was obtained from the Gif collection. It was isolated from the haploid strain *rho*$^+$ *mit*$^+$ 777-3A, α op_1 ade_1 [30] and its mtDNA sequence revealed that the cyt *b* glycine 131 was replaced by a serine [28]. The nuclear recessive op_1 mutation impairs ATP/ADP translocation, which leads to an inability to grow on respiratory substrates, even in the presence of a functional respiratory chain [31]. Therefore the parental strain 777-3A α op_1 ade_1 *rho*$^+$ *mit*$^+$ and mutant W7 were crossed with the *rho*^{0} strain KL14-4A *a* his_1 trp_2 OP_1, which possesses the wild type allele of the op_1 mutation. All the experiments were carried out on diploid strains that were isogenic, with the exception of the cytochrome *b* mutations. Isolation of respiratory competent revertants was as described in [32].

2.2. Medium, growth conditions, in vivo phosphorylation efficiency and preparation of mitochondria

The growth medium contained 2% yeast extract (Difco), 1% bacto-peptone (Difco), 0.12% ammonium sulfate and 2% galactose as the energy source. 1 ml of preculture was used to inoculate toxin flasks containing 500 ml of medium vigorously shaken at 28°C and harvested 48 h later (beginning of the stationary phase), as described previously [33]. Growth yield, phosphorylation efficiency and growth rate were determined as outlined in [34] and [35]. Preparation of mitochondria was performed according to the mechanical method of Guerin et al. [36] with slight modification [33].

2.3. Activities of the whole respiratory chain and of its various segments

All the respiratory activities were carried out on isolated mitochondria. For the whole chain, they were as described by Meunier-Lemesle et al. [33] in the MR3 buffer (0.65 M sorbitol, 10 mM KH_2PO_4, 2 mM EDTA, 0.1 mM $MgCl_2$, 0.3% bovine serum albumin, pH 6.5). The various segment activities described below were measured at 25°C in phosphate buffer (50 mM potassium phosphate, 50 μM EDTA, pH 7.4), using the dual wavelength-stirred reaction cuvette procedure [37]. NADH-ubiquinone reductase activity (segment I) was measured spectrophotometrically by following NADH (0.5 mM) oxidation monitored at the 340/425 nm wavelength pair with DB (0.1 mM) as quinone electron acceptor, in the presence of 2 mM KCN. Complex II activity (succinate-ubiquinone reductase) was measured by DB reduction at 280/325 nm with saturating amounts of succinate (10 mM) as electron donor, in the presence of 2 mM KCN. Complex III, or DBH_2-cytochrome *c* reductase activity, was determined by measuring the reduction of cytochrome *c* (40 μM) at 550 nm using 540 nm as a reference in the presence of KCN (2 mM) with decylubiquinol (50 μM DBH_2) as electron donor. The I_{50} value for inhibitors is defined as the concentration required to reduce the DBH_2-cyt *c* reductase activity by 50% and is expressed in moles of inhibitor per mole of cyt *b* content for each strain. The relative inhibitor titer I'_{50} is the ratio between the I_{50} in a mutated strain and I_{50} obtained with the wild type strain and indicates the resistance of a strain to the inhibitor in comparison with the wild type strain [38]. The combined activities of segment I+III (NADH-cyt *c* reductase) or II+III (succinate-cyt *c* reductase) were measured by monitoring the reduction of cyt *c* at 550/540 nm with NADH or succinate as electron donor, in the presence of 2 mM KCN. Extinction coefficients of 6.22, 16, 18, and 24 mM^{-1} cm^{-1} were used for calculations of NADH, DB, cyt c+c_1 and cyt *b*, respectively.

2.4. Spectral analysis

Optical absorption spectra at room temperature were obtained as described previously [33]. Low temperature spectra were recorded at liquid nitrogen temperature (77 K) using a dual wavelength DW2000 SLM-Aminco spectrophotometer with a slit of 0.2–0.4 nm. Wavelengths were calibrated with a Holmium filter, and the spectra of membranes suspended in MR3 buffer were recorded.

2.5. Redox titrations

Optical redox titrations were carried out at 25°C as described by Dutton [39], with a flow of argon gas, using a dual wavelength DW2000 SLM-Aminco spectrophotometer. Reductive and oxidative titrations were conducted with sodium dithionite and potassium ferricyanide, respectively. Mitochondria were suspended in 50 mM MOPS buffer, pH 7. The following redox mediators were used at a final concentration of 5 μM: potassium ferricyanide, ferrocenemonocarboxylic acid, 1,4-benzoquinone, 2,5-dimethyl-*p*-benzoquinone, 1,2-naphthoquinone, phenazine methosulfate, tetramethyl-*p*-benzoquinone, 2-methyl-1,4-naphthoquinone, 2,5-dihydroxy-*p*-benzoquinone, indigo carmine, 2-hydroxy-1,4-naphthoquinone, anthraquinone-2,6-disulfonate, and anthraquinone-2-sulfonate.

2.6. Presteady-state cytochrome reduction kinetics by the center P and center N pathways

Cyt *b* reduction kinetics were monitored at 562 nm using 575 nm as a reference with a dual wavelength Aminco DW2A spectrophotometer equipped with a rapidly stirred reaction cuvette, as described by Brasseur et al. [37]. NADH (2 mM) or succinate (25 mM) was used as electron donor. Antimycin (20 μM) or myxothiazol (30 μM) was used at saturating levels to observe the center P and center N cyt *b* reduction kinetics, respectively; the 'double kill' was observed when both inhibitors were added (results not shown). Cytochrome $c+c_1$ reduction kinetics by the high potential electron transfer pathway were recorded at 551/540 nm with NADH as electron donor in the presence of 2 mM KCN [40].

2.7. EPR spectra

EPR spectra were recorded at liquid helium temperature on a Bruker ESP 300E X-band spectrometer equipped with an Oxford Instruments liquid helium cryostat and temperature control system. Mitochondria were suspended in 0.65 M sorbitol, 10 mM Tris–HCl, 2 mM EDTA, 0.1% bovine serum albumin, pH 6.5.

2.8. Molecular representation

Molecular representation was carried out using the Swiss-Pdb Viewer software [41] available on the Web (http://www.expasy.ch/spdbv/). The X-ray coordinates of the chicken heart mitochondrial bc_1 complex in the presence of the stigmatellin inhibitor [9] (accession No. 3bcc in the Brookhaven Protein Data Bank) were used to visualize the regions of cytochrome *b* described in this study and to calculate the closest distances between selected atoms.

2.9. Chemicals

Inhibitors were used in the form of stock ethanolic or dimethyl sulfoxide (Me_2SO) solutions. Antimycin and decylubiquinone were obtained from Sigma, myxothiazol from Boehringer and stigmatellin from Fluka. All other chemicals were reagent grade and were purchased from commercial sources.

3. Results

3.1. Characterization of the strains

Non-native intragenic revertant G131S+G260A had been selected from the original cyt *b* respiratory deficient mutant G131S. Whereas the mutant G131S is unable to grow on respiratory substrates (glycerol or ethanol, Table 1), the revertant G131S+G260A is able to grow on these substrates but with a much longer doubling time than that of the wild type strain (19 h and 3 h 5 min on ethanol for the revertant and wild type strain, respectively). In addition to a lower growth rate, the suppressor strain showed a lower growth yield on respiratory substrate ethanol (69% compared to the wild type value). The respiratory deficient mutant G131S grew only by fermentation and exhibited on galactose a lower growth yield (16%) and a higher doubling time (3 h) than the wild type strain (1 h 40 min). The suppressor strain exhibited an intermediate phenotype on galactose with a doubling time of 2 h 15 min and a growth yield of 66% (Table 1), which is in agreement with it being a respiratory competent strain.

Table 1 gives the values of the cytochrome content for the different strains. The results show that the

Table 1
Growth characteristics on respiratory and fermentable substrates, and cytochrome content in the respiratory deficient mutant G131S, in the suppressor mutant G131S+G260A and in the wild type strain

Strains	Growth on respiratory substrates (glycerol, EtOH)	Doubling time on EtOH	Phospho-rylation efficiency on EtOH	Doubling time on galactose	Phosphor-ylation efficiency on galactose	Cytochrome content		
						$c+c_1$	b	$a+a_3$
Wild type (KM91)	GLY^{+++}	3 h 5 min	100	1 h 40 min	100	100	100	100
G131S	GLY^{-}	–	–	3 h	15.8	74	25	96
G131S+G260A	GLY^{+}	19 h	69	2 h 15 min	66	68	71	118

Growth on respiratory (2% EtOH, 2% glycerol) and fermentable (2% galactose) substrates was checked on plates and the doubling time was measured on liquid medium. The phosphorylation efficiency (moles ATP synthesized/mole substrate consumed) was calculated as in [34]. Cytochrome content is expressed as a percentage relative to that found in the wild type. For the wild type strain, total dithionite reduced cytochrome $c+c_1$, b and $a+a_3$ contents are 0.56, 0.46 and 0.14 nmol/mg protein, respectively. Values are expressed as averages based on several experiments.

revertant strain G131S+G260A recovered about 70% of the total dithionite spectral cyt b compared to the wild type strain, whereas the original mutant G131S exhibited only about 25% of total cyt b. The original mutant G131S and its revertant were shown to contain about the same quantity of dithionite reducible cytochromes $c+c_1$ (about 70% compared to the wild type value). No significant difference was observed in the synthesis of cyt aa_3 between the different strains tested. Whereas the bc_1 complex of the cyt b mutant G131S was not properly assembled (cyt b and core protein I deficient [42]), the revertant strain exhibited about 70% of spectral bc_1 complex in the mitochondrial membrane compared to the wild type strain.

3.2. Enzymatic activities in the various segments of the respiratory chain and in the whole chain

Table 2 shows that the succinate oxidase activity was nil in the G131S mutant and amounted to only 17% in the suppressor strain as compared to the wild type strain activity. Succinate and NADH-cyt c reductase activities were nil in the original mutant and attained 26% and 11% in the revertant strain, respectively. As segment I and complex II activities were not drastically modified in this revertant strain (about 100% and 70%, respectively (Table 2)), the defect must be mainly localized at the bc_1 complex level. Indeed, the DBH_2-cyt c reductase activity was

Table 2
Succinate oxidase activity, succinate- and NADH-cyt c reductase activities and activities of the different segments of the respiratory chain

Strains	Succinate oxidase	Succinate-cyt c	NADH-cyt c	Segment I NADH-DB	Complex II succinate-DB	Complex III DBH2-cyt c	
						Activity	T.N.
Wild type	100	100	100	100	100	100	100
G131S	0	0	0	57	6	0	0
G131S+G260A	17	26	11	97	69	11	15

All activities are expressed as percentages of the wild type values. Segment I is used instead of complex I as there is no phosphorylation site associated with NADH-ubiquinone reductase activity in *S. cerevisiae* [43,44]. With the wild type strain, the values obtained were: succinate oxidase, 0.076 μmol O_2 min^{-1} mg^{-1}; succinate-cyt c reductase, 0.24 μmol cyt c reduced min^{-1} mg^{-1}; NADH-cyt c reductase, 0.50 μmol cyt c reduced min^{-1} mg^{-1}; segment I (NADH-DB reductase), 1.48 μmol NADH oxidized min^{-1} mg^{-1}; complex II (succinate-DB reductase), 0.25 μmol DB reduced min^{-1} mg^{-1}; complex III (DBH_2-cyt c reductase), 0.85 μmol cyt c reduced min^{-1} mg^{-1}; complex III turnover number (T.N.), 62 s^{-1}. Values are expressed as averages based on several experiments.

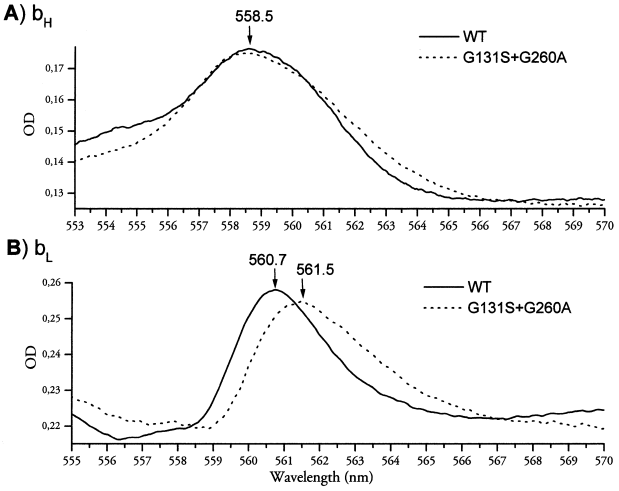

Fig. 1. Optical spectra of hemes b_H and b_L at liquid nitrogen temperature in the wild type and suppressor G131S+G260A strains. Mitochondria were suspended in MR3 buffer at 3.1 mg/ml and 4.2 mg/ml for the wild type (solid line) and suppressor (dashed line) strains, respectively. (A) Heme b_H was obtained from the absorbance difference spectra between succinate reduced and ascorbate reduced mitochondria. (B) Heme b_L was obtained from the absorbance difference spectra of succinate+ascorbate+antimycin minus succinate+ascorbate reduced mitochondria [70].

decreased by approx. 90% in the suppressor strain, although this low activity was enough to sustain a slow growth on respiratory substrates, indicating that the proton translocation associated with this electron transfer is sufficient. The complex II activity of the respiratory deficient mutant G131S was found to be less than 10% compared to the wild type strain, as has already been observed in the case of other respiratory deficient cyt *b* mutants [37,45]. This may be due to a close interaction between the bc_1 and succinate-quinone reductase complexes, as proposed by Bruel et al. [46].

3.3. Optical spectrum analysis of the cyt b_L and b_H hemes in the suppressor and wild type strains

Optical spectra were recorded at room temperature (data not shown) and at liquid nitrogen temperature to enhance the resolution of the peaks. Insofar as heme b_H is concerned, no difference was observed in the revertant strain compared to the wild type strain (Fig. 1A). Conversely, heme b_L was shifted towards the red by 0.8 nm ($\pm$0.1 nm) in the suppressor strain (561.5 nm) compared to the parental strain (560.7 nm) (Fig. 1B). This bathochromic effect was also observed in room temperature experiments in which the suppressor strain exhibited a maximum absorbance for b_L at 566.1 nm, instead of 565.1 nm observed in the wild type strain (data not shown).

We have seen that replacement of the totally conserved residue glycine 131 by serine prevents both the insertion of heme b_L and the assembly of the bc_1 complex [42]. The above results show that the suppressor mutation G260A, in the ef loop, restores the insertion of heme b_L; however, the suppressor strain G131S+G260A presents different characteristics, namely a red shift of about 1 nm of this heme that is obviously due to the presence of the serine in position 131, located only 3 Å from heme b_L (Fig. 5).

3.4. Optical potentiometric redox titrations of the b and c type hemes in the suppressor and wild type strains

Data provided in Fig. 2A could be fit with a single $n=1$ component with a redox midpoint potential of +240 mV for cytochromes c+c_1 in wild type mitochondria, suggesting that cytochromes c and c_1 exhibit similar midpoint potentials. This value is in agreement with those found by both Nelson et al. [47] for the bovine cyt c_1 and Tsai et al. [48] for the yeast cyt c_1 (+232 mV and +268 mV, respectively). No differences were observed between the suppressor and wild type strains for cyt c+c_1. Concerning cyt *b* (Fig. 2B), redox titrations exhibited a typical curve well fit with two $n=1$ components, one with a low midpoint potential (b_L) and a maximum absorption centered at 565 nm which contributes to 40% of the total absorbance, and the other with a higher midpoint potential (b_H) centered at 562 nm, which contributes to about 60% of the total absorbance. In the case of the G131S+G260A revertant, the $E_{m,7}$ for heme b_L was found to be slightly higher (−36 mV) than that of the wild type (−54 mV) (Fig. 2B). No change was observed in the midpoint potential of heme b_H (about 120 mV in both the revertant and wild type strains).

3.5. Kinetics of cyt b and cyt c_1 reduction in the suppressor and wild type strains

According to the Q cycle mechanism [4–6], cyt *b*

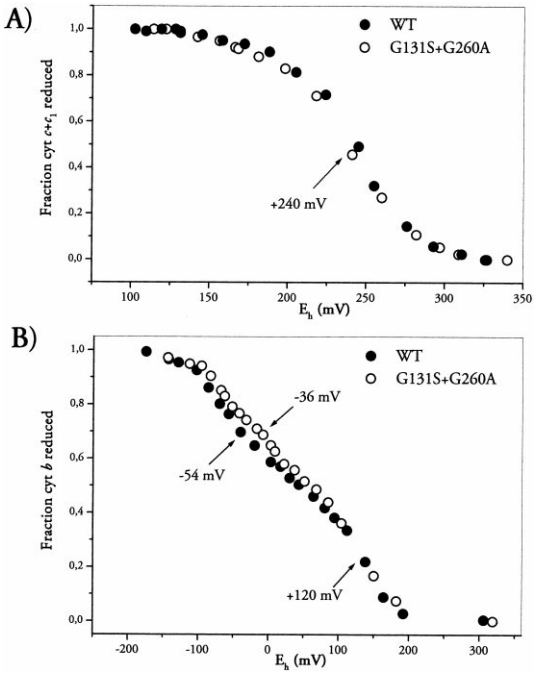

Fig. 2. Redox midpoint potentials of the components of cyt bc_1 complex in mitochondria from the wild type and suppressor G131S+G260A strains. Mitochondria were suspended at a concentration of 4 mg/ml in 50 mM MOPS buffer pH 7 and the experiments were performed as described in Section 2. (A) Cyt c+c_1 redox titration was carried out using the amplitude of the α band at 551 nm as a function of the ambient redox potential and the data were fit with the Nernst equation for one $n=1$ component. Midpoint potential values obtained for the WT (●) and suppressor strains (○) (+240 mV) are indicated in the figure. (B) Cyt b redox titration was carried out using the amplitude of the α band at 563 nm and the data were fit with the Nernst equation for two $n=1$ components. b_L midpoint potential values obtained for the WT and suppressor strains (−54 and −36 mV, respectively), and the b_H midpoint potential (+120 mV for both strains) are indicated in the figure.

can be reduced either by the center P pathway (in the presence of center N inhibitors) or by the thermodynamically unfavorable center N pathway (in the presence of center P inhibitors). In order to investigate which step is modified in the overall steady-state electron transfer from ubiquinol to cytochrome c in the revertant strain, we performed reduction kinetics of both cyt b and cyt c_1 (Fig. 3). These kinetics provide a global value for (1) the rate of arrival and binding of the substrate to its site, (2) the rate of the various electron transfer steps occurring between this binding site and cytochrome b or c_1. The measurements of these reduction kinetics, however, are limited by the lag time of the apparatus, which is of the same order of magnitude as the reduction rate obtained from experiments on the wild type strain. We therefore cannot rule out the possibility that, when the mutated strain exhibits the same reduction kinetic as the parental strain, the corresponding mutation has some effect. Traces presented in Fig. 3 follow apparent first order kinetics and a rate constant was calculated from these kinetics. The percentage of substrate reduction compared to total dithionite reduction of the cytochromes was also informative for the final level of their reduction in the mutant strain as compared to the wild type strain. Reduction of cyt b by the center N pathway was found to be unaffected in the revertant compared to the wild type strain (Fig. 3A), whereas the reduction kinetics of both cyt c+c_1, and cyt b through center P, were found to be affected in the revertant strain G131S+G260A (Fig. 3B,C). The cyt b reduction kinetics through center P, which exhibited an apparent first order rate constant, decreased by at least 60% compared to the wild type strain and the level of substrate reducible cyt b as compared to the total dithionite reducible cyt b is diminished by 30% (46% in the revertant versus 76% in the wild type strain, results not shown). Fig. 3C shows that the reduction kinetics of the high potential pathway (involving both the FeS

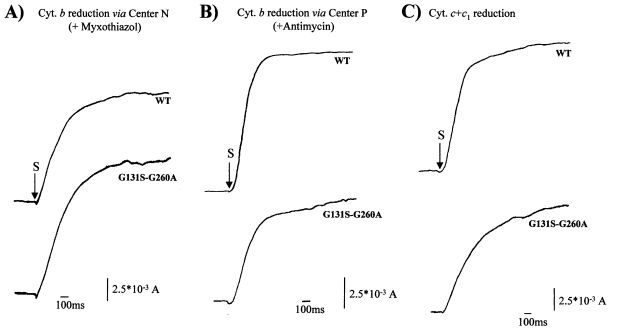

Fig. 3. Reduction kinetics of cyt b via the center N and center P pathways and reduction kinetics of cyt c_1 in the wild type and suppressor G131S+G260A strains. (A) Cyt b reduction kinetics via center N (in the presence of the center P inhibitor myxothiazol). NADH (2 mM) was used as substrate (S) to initiate cyt reduction. (B) Cyt b reduction kinetics via center P (in the presence of the center N inhibitor antimycin). (C) Cyt c+c_1 reduction kinetics (in the presence of KCN). Reactions were followed at 562/575 nm and 551/540 nm for the cyt b and cyt c+c_1 reductions, respectively. The same amount of substrate reducible cyt b (A,B) or cyt c+c_1 (C) was present in the wild type and suppressor strains in each experiment.

Rieske protein and cyt c_1) by the first electron from the Q_P bound quinol was also diminished by more than 60% in the revertant strain compared to the wild type one. The level of cyt c+c_1 reduction decreased by only 10% (84% in the suppressor versus 93% in the wild type strain) at the end of the reduction.

These results show that the revertant strain is affected in the electron transfer steps at the Q_P site of the bc_1 complex.

3.6. Catalytic efficiency and inhibitor binding at the Q_P site

The bc_1 complex steady-state activity has been described as a ping-pong mechanism in which ubiquinol and cyt c interact with two independent sites. In order to determine the apparent second order rate constant (k_{min}) that characterizes the arrival and binding of the substrate to its site [49,50], we performed steady-state DBH_2-cyt c reductase activities by varying the concentration of the reducing substrate DBH_2 while maintaining the other substrate, the soluble horse heart cyt c, at saturating levels. The constant k_{min} (Table 3) can be calculated from the ratio of maximal turnover to apparent K_m (it should be borne in mind that the K_m is a complex parameter in the ping-pong mechanism). For the revertant strain, the k_{min} was found to be 14 times lower than for the wild type strain (1.86×10^6 versus 26.8×10^6 M^{-1} s^{-1}), which indicates that the kinetic interaction of ubiquinol with the bc_1 complex Q_P site is affected. As the binding site for ubiquinol is supposed to at least overlap with those of certain inhibitors such as myxothiazol and stigmatellin, within a buried and hydrophobic region of cyt b [51], we subsequently measured the I_{50} inhibitor titers for myxothiazol and stigmatellin (concentration of inhibitor required to reduce the DBH_2-cyt c reductase activity by 50%) in both the mutant and wild type strains. The relative inhibitor titer values ($I^r_{50} = I_{50}$ mutant/I_{50} wild type) reveal that the revertant strain exhibited only a slight resistance towards myxothiazol ($I^r_{50} = 1.37$) and a low sensitivity towards stigmatellin ($I^r_{50} = 0.54$) (Table 3). These data show that, despite the fact that the quinol interaction at the Q_P site was modified in the revertant strain, the interaction of the Q_P inhibitors myxothiazol and stigmatellin with this site was poorly affected.

3.7. EPR characterization of the Q_P site occupancy

The Q_P site occupancy was monitored by EPR spectroscopy using the characteristic interaction between the [2Fe–2S] cluster of the FeS Rieske protein and the quinone/quinol binding at the Q_P site. It is well known that a g_x signal centered at $g = 1.80$ is observed when the Q pool is fully oxidized (E_h around 200 mV) and that this signal shifts to a lower g_x value of around 1.77 when the Q pool is fully reduced (E_h around 0 mV) [18,52,53]. A value of $g_x = 1.78$ is observed when the Q_P site is occupied by the chromone inhibitor stigmatellin [54]. When the Q_P site is empty, due to either a mutation or extraction of quinones, the value of the g_x signal is centered at $g = 1.76$ [18]. Fig. 4A shows that, in the case of the wild type strain, an EPR spectrum (typical of the presence of the FeS Rieske protein) was obtained when the sample was reduced with ascorbate: a g_y peak at $g = 1.90$ and a g_x trough centered

Table 3
Catalytic properties of the bc_1 complex with the substrate DBH_2 (V_{max}, K_m, k_{min}) and resistance to inhibitors myxothiazol and stigmatellin in the wild type and revertant strains

Strains	V_{max} (s^{-1})	K_m DBH_2 (M)	$k_{min} = V_{max}/K_m$(M^{-1} s^{-1})	I^r_{50} for myxothiazol	I^r_{50} for stigmatellin
Wild type (KM91)	62.9	2.35×10^{-6}	26.8×10^6	1	1
G131S+G260A	6.45	3.45×10^{-6}	1.86×10^6	1.37	0.54

V_{max} represents the maximum DBH_2-cyt c reductase activity (mol cyt c reduced s^{-1}/mol cyt b) measured at 550/540 nm with a dual wavelength spectrophotometer. K_m for DBH_2 was deduced from the titration of the cyt c reductase activity with increasing amounts of the substrate DBH_2 and plotted with a Lineweaver–Burk representation (not shown). k_{min} (V_{max}/K_m) represents the enzyme catalytic efficiency for the substrate. The inhibitor titers I_{50} (concentration of inhibitor required to reduce the DBH_2-cyt c reductase activity by 50%) were 0.84 mol myxothiazol/mol cyt b and 0.38 mol stigmatellin/mol cyt b in the wild type strain. The relative inhibitor titer (I^r_{50}) is the ratio of I_{50} in the mutated strain relative to that in the wild type strain.

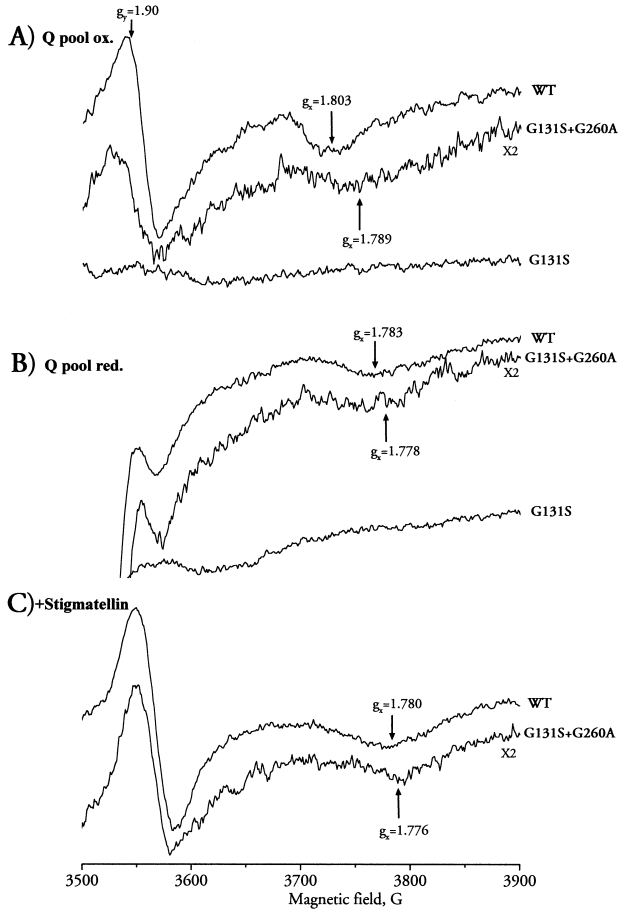

Fig. 4. Q_P site occupancy probed by EPR spectra of the Rieske [2Fe–2S] cluster. (A) EPR spectra were recorded after mitochondria were reduced with 10 mM ascorbate (Q pool oxidized) or (B) with a few grains of dithionite (Q pool completely reduced). (C) The inhibitor stigmatellin was added at a final concentration of 20 μM. Note that the scale is different (×2) for the revertant G131S+G260A strain. Mitochondrial protein concentration was 25, 23 and 29 mg/ml for the wild type strain, the revertant G131S+G260A and original mutant G131S, respectively. Spectra obtained in the presence of dithionite (B) exhibited a lower g_y signal at $g = 1.90$ due to a negative contribution of the complex II iron–sulfur clusters. EPR conditions were as follows: temperature, 15 K; microwave frequency, 9.42 GHz; microwave power, 6.3 mW; modulation frequency, 100 kHz; modulation amplitude, 1.6 milliteslas (mT).

at $g = 1.803$. This latter signal is characteristic of a Q_P site fully occupied with oxidized quinone. In the case of the revertant strain G131S+G260A, the amplitude of the g_y signal was smaller than that of the wild type strain (Fig. 4A,C), which reflects a smaller quantity of EPR detectable FeS protein (about 50% compared to the wild type); the g_x signal was less pronounced and shifted to a lower value of $g_x = 1.789$, thus indicating a partially empty Q_P site (Fig. 4A). In the case of the original G131S mutant, almost no g_y signal was detected, both with ascorbate and dithionite reduced sample (Fig. 4A,B), which confirms that this mutant presents a bc_1 complex non-assembly phenotype. When samples were reduced with dithionite (Fig. 4B), the Q pool was fully reduced and the g_x signal was shifted from $g_x = 1.803$ to a value of $g_x = 1.783$ in the wild type strain, thus showing the response of the EPR [2Fe–2S] cluster g_x signal to the redox state of the Q pool. In the suppressor strain G131S+G260A, the g_x signal shifted less, going from 1.789 to a value of 1.778, most likely due to the low level of quinone occupancy in the Q_P site of this revertant strain. This result is in agreement with the results found in the previous section, where a low catalytic efficiency for quinol was found in the suppressor strain with a k_{min} that had decreased by more than one order of magnitude (Table 3). However, this revertant was still able to bind the Q_P site inhibitor stigmatellin as shown by a deeper g_x trough centered at $g_x = 1.776$ (Fig. 4C). These data are also in accordance with the inhibitor titration experiments performed on this strain, which revealed that the suppressor strain was not resistant to stigmatellin, being in fact slightly more sensitive to this inhibitor (Table 3).

Taken as a whole, the data indicate that the suppressor mutation G260A restores the assembly of the bc_1 complex compared to the original respiratory deficient mutant G131S. They also imply that the low steady-state quinol cyt *c* reductase activity of the revertant strain is due to an electron transfer impairment at the level of the Q_P site, which is at least partially related to a weaker quinol binding at the quinol oxidizing site of the bc_1 complex where both cyt *b* positions G131 and G260 are localized (see Fig. 5).

4. Discussion

In this study, we addressed the question of whether an intragenic suppressor mutation at a distinct position from the original mutation could compensate mutation at the totally conserved position 131 which prevents the assembly of the bc_1 complex.

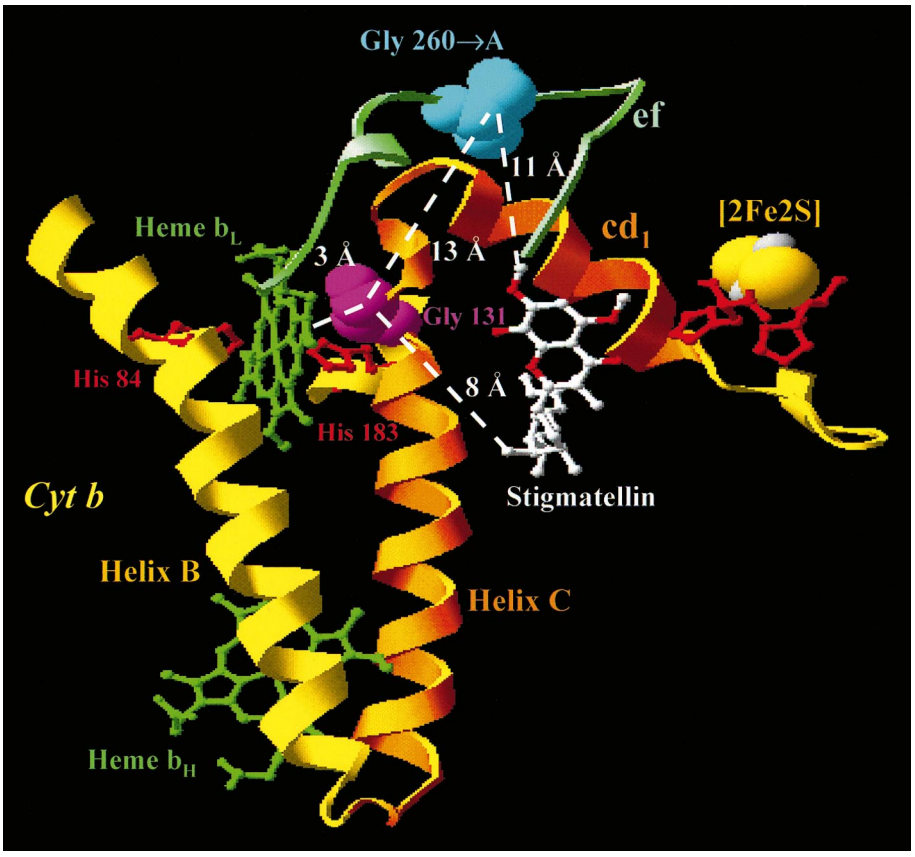

Fig. 5. Model of the cyt *b* region showing the positions G131 and G260 in the three-dimensional structure of the chicken heart mitochondrial bc_1 complex. Cyt *b* G131 (pink) is one of the four conserved glycines involved in heme packing [24] and is located at the C-terminal part of the transmembrane helix C. The intragenic suppressor mutation G260A (blue colored) is located in the ef loop (light green) above the amphipathic helix cd_1 lying on the top of the membrane. For clarity, only two of the eight transmembrane cyt *b* helices of one bc_1 complex monomer are depicted, as are the two histidine (His161 and His141 in red) ligands of the [2Fe2S] cluster of the FeS Rieske protein (gray an yellow balls). Heme b_L, which is red shifted in the suppressor strain, and heme b_H are colored in green. The two histidine (His84 and His183, chicken numbering) ligands of heme b_L located in helix B and D, respectively, are depicted in red. Distances are 13 Å between G131 and G260, 3 Å between G131 and heme b_L, 8 Å between G131 and the hydrophobic tail of the center P inhibitor stigmatellin (CPK colors), and 11 Å between G260 and the polar head of stigmatellin. The coordinates of the chicken heart mitochondrial bc_1 complex in the presence of the inhibitor stigmatellin were used for this figure (accession No. 3bcc in the Brookhaven Protein Data Bank).

We also examined how such a compensation might occur. A respiratory competent strain was isolated from the respiratory deficient mutant G131S; the intragenic suppressor mutation was localized on cyt *b* at position 260 where the glycine was replaced by an alanine, leading to the revertant strain G131S+G260A. Whereas the original mutant G131S presented a non-assembled bc_1 complex with less than 25% of total *b* type cytochromes and no Core I and Rieske FeS protein, the revertant strain exhibited an assembled bc_1 complex with about 70% of the *b* and *c* type cytochromes and about 50% of the FeS protein (Table 1 and Fig. 4). The low bc_1 complex activity of the revertant strain (about 15% of wild type enzyme turnover) (Table 2) was enough to sustain slow growth, indicating that the coupling between electron transfer and proton translocation was maintained in this revertant strain. It should be noted that the cyt *b* respiratory deficient mutant G131S exhibited less than 10% of the complex II activity, thus suggesting either a direct and close interaction between complexes II and III and/or a downregulation of expression of complex II in respiratory deficient complex III mutants, as has already been proposed [37,45,46].

We have seen that, due to their small side chains,

the four totally conserved glycines G131 and G47, as well as G117 and G33, allow the correct insertion of heme b_L and heme b_H, respectively. Fig. 1 shows that heme b_L was red shifted by about 1 nm in the G131S+G260A suppressor strain, certainly due to the presence of the longer and protonated side chain of serine replacing the smaller amino acid glycine in position 131, close to heme b_L. It is to be noted that a similar result was obtained in the case of the cyt *b* revertant strain G33A isolated from the non-assembly mutant G33D. This suppressor strain [25] exhibits a bathochromic effect of 1.5 nm for heme b_H [26], from which the totally conserved G33 is distant by only 3.5 Å.

Redox titration experiments showed that the $E_{m,7}$ of heme b_L in the revertant G131S+G260A was slightly higher (−36 mV) than that of the wild type (−54 mV) (Fig. 2B). However, this difference of 18 mV was not considered to be sufficiently large to be the only factor responsible for the low steady-state ubiquinol-cytochrome *c* reductase activity in the revertant strain. In this study, the $E_{m,7}$ values for hemes b_H and b_L found for the wild type yeast bc_1 complex were similar to those reported for the mitochondrial bc_1 complex (+19 and +109 mV for b_L and b_H, respectively, in yeast complex III [56]; −34 and +93 mV for b_L and b_H, respectively, in bovine bc_1 complex [47]) and are higher than those found in the photosynthetic bacterium *R. capsulatus* [29] (−126 and +71 mV for b_L and b_H, respectively). Saribas et al. [29] have shown that rather small and non-polar amino acid substitutions like alanine and valine obtained by site directed mutagenesis at the conserved glycine 146 in *R. capsulatus* (corresponding to glycine 131 in *S. cerevisiae*) affect neither the assembly of the bc_1 complex nor the heme b_L and b_H midpoint potentials. Thus, it appears that a small and/or non-polar residue is required to allow correct heme b_L packing. In the suppressor strain G131S+G260A, no effect was detected on the Q_N site; conversely, the kinetics of electron transfer involving the Q_P site were found to be affected, as was demonstrated by the slower cyt *b* and cyt c_1 reduction kinetics by the low and high potential pathways, respectively (Fig. 3B,C). The decreased k_{min} (Table 3) as well as the EPR results (which showed that the revertant strain exhibited a partially empty Q_P site (Fig. 4)), suggest a modified interaction of the substrate quinol at the Q_P site. The response to the redox state of the quinol pool was therefore weak in the revertant strain. These data show that the quinol/quinone interaction in the bc_1 complex of the revertant strain was modified and might at least partially explain the slower cyt *b* and c_1 reduction kinetics and the low steady-state DBH_2-cyt *c* reductase activity observed in the suppressor strain. Saribas et al. [29] have shown that alanine and valine substitutions at glycine 146 in *R. capsulatus* (G131 in yeast) lead to an unoccupied Q_P site. As the suppressor mutation G260A restored the deficiency due to a serine mutation in position 131, it seems likely that the G131S mutation is directly or indirectly responsible for the low quinol occupancy at the Q_P site, probably by locally modifying the transmembrane helix C (and then its interaction with heme b_L) and thus modifying the quinol binding site. However, it is not possible to discriminate which of the distal and proximal quinol/semiquinone binding sites in the Crofts model [22,51,57] is affected nor is it possible to ascertain which of the two Q_{Os} and Q_{Ow} quinone binding sites in the model of Ding et al. [18] is affected. It should be noted that the stigmatellin binding in the revertant strain was not modified and no resistance or sensitivity was found for the Q_P site inhibitor myxothiazol (Table 3 and Fig. 4C). These data are in agreement with the distance values between the inhibitors and positions G131 and G260 in the three-dimensional structure of the bc_1 complex: glycine 131 and glycine 260 were found to be 6.5 Å and 10.5 Å away from the closest atom of the methoxyacrylate group of myxothiazol, respectively. Concerning stigmatellin, an inhibitor of the chromone family [58], glycine 131 was found to be at 8.1 Å from the closest atom in the inhibitor hydrophobic alkenyl tail and glycine 260 is at 11 Å from the closest atom in the dimethoxyhydroxychromone system of the stigmatellin polar head (Fig. 5). Thus, our results show that mutations at positions 131 and 260 are not involved in the stigmatellin and myxothiazol binding domains, but mutation G131S modifies quinol binding. This suggests that the quinol and stigmatellin binding domains are not strictly identical. The modified region of the quinol binding domain probably does not belong to the shared volume by stigmatellin and myxothiazol, which is located in the more buried region of cyt *b* where both the hy-

drophobic tails of the inhibitors are found [11,51]. The effect seen on the k_{min} and the EPR spectra for quinol binding may be due to either an indirect effect linked to a structural modification of the ef loop (which includes position 260), thus leading to an impairment of the catalytic oxidation of ubiquinol by the FeS protein when this latter protein is in the proximal position close to cyt *b*, in contact with the ef loop, or to a repositioning of the transmembrane helix C to accommodate the serine in position 131, with a subsequent effect on quinol binding. Saribas et al. [29] reported that G146A,V mutations impaired the cyt *b* and c_1 reduction kinetics by the Q_P site, which is unoccupied by quinol/quinone, whereas stigmatellin binding was not affected in these mutants, as was observed in the present study. The EPR g_z signal of heme b_L was modified in these mutants, indicating that an increase in the size of the amino acid side chain at position 146 (131 in yeast) perturbs the spatial conformation of heme b_L. In the same way, optical spectra have revealed a perturbation of heme b_L, the absorption maximum of which is red shifted in the revertant.

Analyzing the theoretically possible substitutions at position 131, it was not possible, from the original G131S mutant, to obtain reversions with small and non-polar amino acids such as alanine or valine by a single base substitution. Only charged amino acids or those bigger than serine could have been obtained by a single base change; however, they likely induce a non-assembly of the complex and thus the non-selection of these revertants on respiratory substrates. The suppressor mutation at position 260 was found with a low reversion frequency (about 10^{-9}), still higher, however, than the frequency of a double base mutation necessary to obtain an alanine or valine in position 131. In the bc_1 complex structure, modeling mutation G131S revealed that amino acids with long side chains cannot be tolerated at position 131 (in pink in Fig. 5) and would clash with either heme b_L, which is located only 3 Å away, or the cyt b_L histidine ligand 183 (in red), which is located only 2.5 Å from the conserved glycine. Surprisingly, analysis of the initial and suppressor mutations in the three-dimensional structure of the bc_1 complex (Fig. 5) showed that the suppressor mutation was located far from both the initial mutation (13 Å from G131) and heme b_L. This long distance interaction cannot be explained in the context of the dimeric bc_1 complex as the distance between the original mutation, in one monomer, and the suppressor mutation, in the other monomer, was greater than 25 Å. It has been suggested that a movement of the head domain of the FeS Rieske protein is involved in rapid electron transfer by domain movement [8–11,22]. In the *b* state, the ef loop is in contact with the FeS protein. Modifying the ef loop could therefore change both the docking surface with the Rieske protein [22] and, as a result, the quinol oxidation at the Q_P site. This may explain the quinol binding deficiency observed in the revertant strain.

In previous reports, intragenic and extragenic suppressor mutations have been described and studied in yeast ([25,26,32,35,37,38,45,59–63,71] and *R. capsulatus* [12,64,65] bc_1 complexes (see [66] for review) and analyses of mutant/revertant pairs have been used to tentatively propose a topology of the protein. It should be stressed that obtaining second site suppressor mutations can lead to unexpected results, which are always functionally relevant because they are 'naturally' selected. However, it should also be kept in mind that suppressor mutations do not always reveal proximal interactions. Knowing the structure of the bc_1 complex, we analyzed the localization of several intragenic suppressor mutations of the yeast bc_1 complex and found that in some cases, although the reversion is distant in the sequence from the original mutation, both positions are found to be in close proximity within the structure (for example the cyt *b* G137E original mutation and its reversion N256K are only 3.4 Å apart, C133Y and I176S are separated by only 4 Å). Conversely, examples of long distance interactions of up to 46 Å between cyt *b*, cyt c_1 and the FeS protein were found in *R. capsulatus* [64]. Similarly, more than 20 Å separates the cluster and the tether regions of the FeS protein in the mutant/revertant pairs described in [12]. In the bacterial reaction center, suppressor mutations have been obtained and have revealed long distance interactions [67,68]. In the same way, long distance interactions have been found to occur in the transmembrane subunit I of cytochrome oxidase in *S. cerevisiae* [69].

Glycine is totally conserved in position 131, thus allowing (1) the insertion of heme b_L, (2) the positioning of the adjacent highly conserved Tyr 132 involved in electron transfer [65], and (3) the position-

ing of b_L heme ligand His 183. Interestingly, glycine 260 is only found in *S. cerevisiae*. Indeed, it is replaced by a valine in protozoa and an alanine is naturally present in all other organisms, as it is in subunit IV of the b_6f complex [55]. A methyl group in position 260 (glycine to alanine) is thus sufficient to allow the assembly of the G131S mutant bc_1 complex in *S. cerevisiae*. Indeed, in the bc_1 complex structures, the side chain of alanine 260 in the ef loop faces the amphipathic helix cd_1 (Fig. 5) and is located 3.4 Å from the closest atom of G137, 4 Å from W136 (Y136 in yeast) and 3.6 Å from F141 (H141 in yeast), all of which belong to the cd_1 helix. It is thus possible that an additional methyl group in position 260 displaces the cd_1 helix, and consequently the transmembrane helix C, to create a volume necessary for both the positioning of the serine side chain in position 131 and the insertion of heme b_L.

In conclusion, this study reveals a long distance interaction in the bc_1 complex between an intramembrane helix and an intermembrane loop of cyt *b*. Despite the fact that glycine 131 is one of the four totally conserved glycines, and that it is packed in the membrane against both heme b_L and the histidine coordinating this heme, this study shows that it is possible to find a suppressor mutation at a long distance (13 Å) from the original mutation, in a non-membranous part of cyt *b*. This suggests subtle functional modifications at the Q_P site that are difficult to predict through a mere analysis of the bc_1 complex structure. Moreover, it is noteworthy that the only suppressor mutation found from this G131S mutant is a long distance reversion. Indeed, neither same site reversions at position 131 nor proximal second site suppressor mutations were obtained in the case of the G131S mutant, as is usually the case in the study of other couple mutants/revertants.

In a more general way, this study shows that a slight modification at a non-critical position (G260A) may induce a succession of slightly modified interactions between closely related residues, leading to an important change at a critical and distal residue (G131).

Acknowledgements

The authors would like to thank M. Johnson for looking over the English and the groups of P. Bertrand and W. Nitschke for advices with the EPR machine.

References

[1] U. Brandt, B. Trumpower, Crit. Rev. Biochem. Mol. Biol. 29 (1994) 165–197.
[2] K.A. Gray, F. Daldal, in: R.E. Blankenship, M.T. Madigan, C. Bauer (Eds.), Anoxygenic Photosynthetic Bacteria, Kluwer Academic Publishers, Dordrecht, 1995, pp. 747–774.
[3] W.A. Cramer, G.M. Soriano, M. Ponomarev, D. Huang, H. Zhang, S.E. Martinez, J.L. Smith, Annu. Rev. Plant Physiol. Plant Mol. Biol. 47 (1996) 477–508.
[4] P. Mitchell, FEBS Lett. 59 (1975) 137–139.
[5] P. Mitchell, J. Theor. Biol. 62 (1976) 327–367.
[6] B.L. Trumpower, J. Biol. Chem. 265 (1990) 11409–11412.
[7] B.L. Trumpower, Microbiol. Rev. 54 (1990) 101–129.
[8] D. Xia, C.A. Yu, H. Kim, J.Z. Xia, A.M. Kachurin, L. Zhang, L. Yu, J. Deisenhofer, Science 277 (1997) 60–66.
[9] Z. Zhang, L. Huang, V.M. Shulmeister, Y.I. Chi, K.K. Kim, L.W. Hung, A.R. Crofts, E.A. Berry, S.H. Kim, Nature 392 (1998) 677–684.
[10] S. Iwata, J.W. Lee, K. Okada, J.K. Lee, M. Iwata, B. Rasmussen, T.A. Link, S. Ramaswamy, B.K. Jap, Science 281 (1998) 64–71.
[11] H. Kim, D. Xia, C.A. Yu, J.Z. Xia, A.M. Kachurin, L. Zhang, L. Yu, J. Deisenhofer, Proc. Natl. Acad. Sci. USA 95 (1998) 8026–8033.
[12] G. Brasseur, V. Sled, U. Liebl, T. Ohnishi, F. Daldal, Biochemistry 36 (1997) 11685–11696.
[13] E. Darrouzet, M. Valkova-Valchanova, C.C. Moser, P.L. Dutton, F. Daldal, Proc. Natl. Acad. Sci. USA 97 (2000) 4567–4572.
[14] H. Tian, L. Yu, M.W. Mather, C.A. Yu, J. Biol. Chem. 273 (1998) 27953–27959.
[15] H. Tian, S. White, L. Yu, C.A. Yu, J. Biol. Chem. 274 (1999) 7146–7152.
[16] C. Hunte, J. Koepke, C. Lange, T. Robmanith, H. Michel, Structure 8 (2000) 669–684.
[17] A.R. Crofts, S.W. Meinhardt, K.R. Jones, M. Snozzi, Biochim. Biophys. Acta 723 (1983) 202–218.
[18] H. Ding, D.E. Robertson, F. Daldal, P.L. Dutton, Biochemistry 31 (1992) 3144–3158.
[19] U. Brandt, FEBS Lett. 387 (1996) 1–6.
[20] T.A. Link, FEBS Lett. 412 (1997) 257–264.
[21] S. Junemann, P. Heathcote, P.R. Rich, J. Biol. Chem. 273 (1998) 21603–21607.
[22] A.R. Crofts, M. Guergova-Kuras, L. Huang, R. Kuras, Z. Zhang, E.A. Berry, Biochemistry 38 (1999) 15791–15806.
[23] C.H. Snyder, E.B. Gutierrez-Cirlos, B.L. Trumpower, J. Biol. Chem. 275 (2000) 13535–13541.
[24] T. Tron, M. Crimi, A.-M. Colson, M. Degli-Esposti, Eur. J. Biochem. 199 (1991) 753–760.

[25] J.-Y. Coppee, N. Tokutake, D. Marc, J.-P. di Rago, H. Miyoshi, A.-M. Colson, FEBS Lett. 339 (1994) 1–6.
[26] G. Brasseur, P. Brivet-Chevillotte, Eur. J. Biochem. 230 (1995) 1118–1124.
[27] C.H. Yun, Z. Wang, A.R. Crofts, R.B. Gennis, J. Biol. Chem. 267 (1992) 5901–5909.
[28] P. Brivet-Chevillotte, J.-P. di Rago, FEBS Lett. 255 (1989) 5–9.
[29] A.S. Saribas, H. Ding, P.L. Dutton, F. Daldal, Biochim. Biophys. Acta 1319 (1997) 99–108.
[30] Z. Kotylak, P.P. Slonimski, in: W. Bandlow, R.J. Schweyen, K. Wolf, F. Kaudewitz (Eds.), Mitochondria, Genetics and Biogenesis of Mitochondria, Walter de Gruyter, Berlin, 1977, pp. 161–172.
[31] L. Kovac, T.M. Lachowicz, P.P. Slonimski, Science 158 (1967) 1564–1567.
[32] J.-P. di Rago, P. Netter, P.P. Slonimski, J. Biol. Chem. 265 (1990) 3332–3339.
[33] D. Meunier-Lemesle, P. Chevillotte-Brivet, P. Pajot, Eur. J. Biochem. 111 (1980) 151–159.
[34] P. Chevillotte-Brivet, D. Meunier-Lemesle, Eur. J. Biochem. 111 (1980) 161–169.
[35] J.-Y. Coppee, G. Brasseur, P. Brivet-Chevillotte, A.-M. Colson, J. Biol. Chem. 269 (1994) 4221–4226.
[36] B. Guerin, P. Labbe, M. Somlo, Methods Enzymol. 55 (1979) 149–159.
[37] G. Brasseur, J.Y. Coppée, A.-M. Colson, P. Brivet-Chevillotte, J. Biol. Chem. 270 (1995) 29356–29364.
[38] G. Brasseur, P. Brivet-Chevillotte, FEBS Lett. 354 (1994) 23–29.
[39] P.L. Dutton, Methods Enzymol. 54 (1978) 411–435.
[40] G. Brasseur, P. Tron, G. Dujardin, P.P. Slonimski, P. Brivet-Chevillotte, Eur. J. Biochem. 246 (1997) 103–111.
[41] N. Guex, M.C. Peitsch, Electrophoresis 18 (1997) 2714–2723.
[42] P. Chevillotte-Brivet, G. Salou, D. Meunier-Lemesle, Curr. Genet. 12 (1987) 111–117.
[43] S. de Vries, L.A. Grivell, Eur. J. Biochem. 176 (1988) 377–384.
[44] T. Ohnishi, FEBS Lett. 24 (1972) 305–309.
[45] C. Bruel, J.-P. di Rago, P.P. Slonimski, D. Lemesle-Meunier, J. Biol. Chem. 270 (1995) 22321–22328.
[46] C. Bruel, R. Brasseur, B.L. Trumpower, J. Bioenerg. Biomembr. 28 (1996) 59–68.
[47] B.D. Nelson, P. Gellerfors, Biochim. Biophys. Acta 357 (1974) 358–364.
[48] A.L. Tsai, G. Palmer, Biochim. Biophys. Acta 722 (1983) 349–363.
[49] F.B. Rudolph, H.J. Fromm, Methods Enzymol. 63 (1979) 138–159.
[50] M. Degli-Esposti, G. Lenaz, Arch. Biochem. Biophys. 289 (1991) 303–312.
[51] A.R. Crofts, B. Barquera, R.B. Gennis, R. Kuras, M. Guergova-Kuras, E.A. Berry, Biochemistry 38 (1999) 15807–15826.
[52] K. Matsuura, J.R. Bowyer, T. Ohnishi, P.L. Dutton, J. Biol. Chem. 258 (1983) 1571–1579.
[53] H. Ding, F. Daldal, P.L. Dutton, Biochemistry 34 (1995) 15997–16003.
[54] G. von Jagow, T. Ohnishi, FEBS Lett. 185 (1985) 311–315.
[55] M. Degli-Esposti, S. De Vries, M. Crimi, A. Ghelli, T. Patarnello, A. Meyer, Biochim. Biophys. Acta 1143 (1993) 243–271.
[56] A.L. Tsai, R. Kauten, G. Palmer, Biochim. Biophys. Acta 806 (1985) 418–426.
[57] A.R. Crofts, S. Hong, Z. Zhang, E.A. Berry, Biochemistry 38 (1999) 15827–15839.
[58] G. von Jagow, T.A. Link, Methods Enzymol. 126 (1986) 253–271.
[59] J.-P. di Rago, P. Netter, P.P. Slonimski, J. Biol. Chem. 265 (1990) 15750–15757.
[60] J.-P. di Rago, S. Hermann-Le Denmat, F. Pâques, F.P. Risler, P. Netter, P.P. Slonimski, J. Mol. Biol. 248 (1995) 804–811.
[61] C. Bruel, S. Manon, M. Guerin, D. Lemesle-Meunier, J. Bioenerg. Biomembr. 27 (1995) 527–539.
[62] C. Bruel, D. Lemesle-Meunier, Biochem. Soc. Trans. 22 (1994) 61S.
[63] G. Brasseur, P. Brivet-Chevillotte, Biochem. Soc. Trans. 22 (1994) 60S.
[64] A.S. Saribas, M. Valkova-Valchanova, M.K. Tokito, Z. Zhang, E.A. Berry, F. Daldal, Biochemistry 37 (1998) 8105–8114.
[65] A.S. Saribas, H. Ding, P.L. Dutton, F. Daldal, Biochemistry 34 (1995) 16004–16012.
[66] G. Brasseur, A.S. Saribas, F. Daldal, Biochim. Biophys. Acta 1275 (1996) 61–69.
[67] J. Miksovska, M. Schiffer, D.K. Hanson, P. Sebban, Proc. Natl. Acad. Sci. USA 96 (1999) 14348–14353.
[68] P. Sebban, P. Maroti, M. Schiffer, D.K. Hanson, Biochemistry 34 (1995) 8390–8397.
[69] B. Meunier, P.R. Rich, J. Mol. Biol. 283 (1998) 727–730.
[70] D. Lemesle-Meunier, P. Brivet-Chevillotte, J.-P. di Rago, P.-P. Slonimski, C. Bruel, T. Tron, N. Forget, J. Biol. Chem. 268 (1993) 15626–15632.
[71] J.-P. di Rago, P.-P. Slonimski, in: S. Papa, F. Guerrieri, J. Tager (Eds.), Frontiers of Cellular Bioenergetics: Molecular Biology, Biochemistry and Physiopathology, Kluwer Academic Plenum Publ. Corp., New York, 1999, pp. 593–619.